Journal of Material Cycles and Waste Management (2023) 25:157–170
https://doi.org/10.1007/s10163-022-01520-8

ORIGINAL ARTICLE

The improvement of strength and microstructural properties of fly ash-based geopolymer by adding elemental aluminum powder

Uğur Durak[1]

Received: 26 June 2022 / Accepted: 28 September 2022 / Published online: 9 October 2022

Abstract

In this study, 1, 2, and 3% micronized aluminum powder were used by replacing with fly ash to improve the properties of F class fly ash-based geopolymer mortar samples. The produced geopolymer mortar samples were heat cured at 60, 70, and 80 °C temperatures for 24 and 48 h. Following heat curing, the unit weights, flexural, and compressive strengths of the hardened geopolymer mortar samples were determined. In addition, XRD, FESEM, EDX, and isothermal calorimetry experiments were carried out to examine the changes in the microstructure with the addition of aluminum in detail. Based on the results obtained, it was observed that the substitution of micronized aluminum powder slightly decreased the workability of the geopolymer mortar samples. Moreover, it increased the flexural and compressive strength significantly (more than double) for 24 h heat curing. The XRD, FESEM, EDX and isothermal calorimetry experiments showed that the substitution of aluminum powder in the fly ash-based geopolymer system increased the geopolymerization reactions and, in comparison to the reference sample, created sodalite minerals in the microstructure. Therefore, it was concluded that the aluminum powder substitution transforms the microstructure into a stronger structure, thus improving the mechanical properties.

Graphical abstract

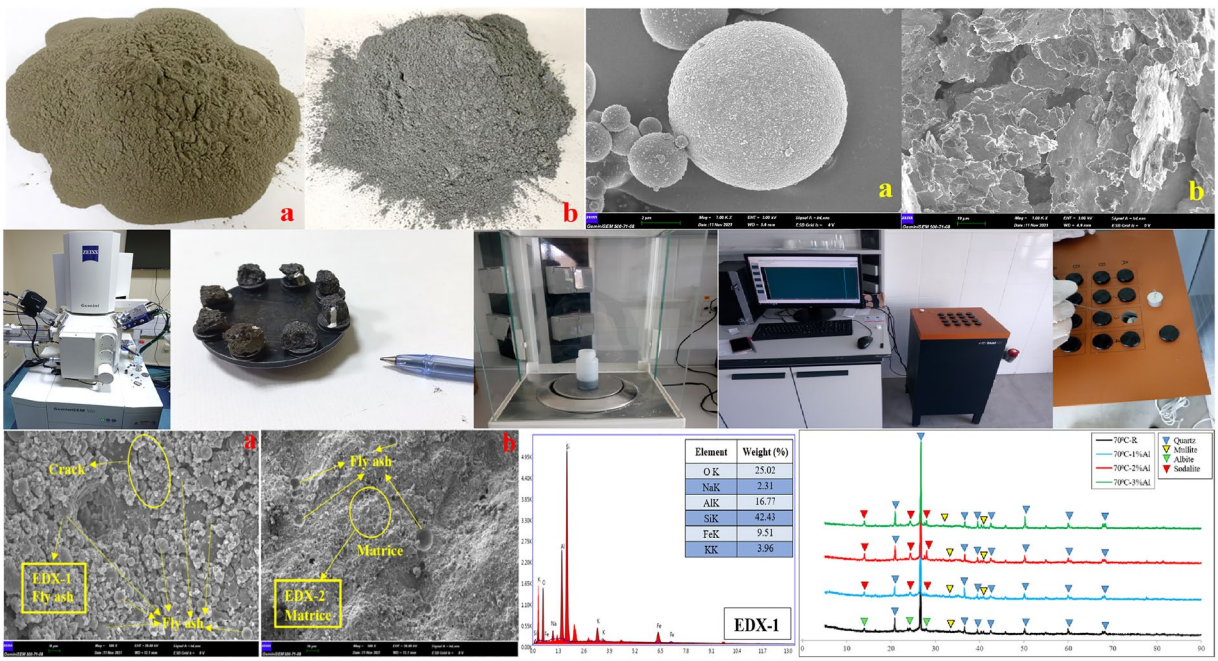

Keywords Fly ash · Aluminum · Geopolymer · Microstructure · Sodalite

Extended author information available on the last page of the article

Introduction

Portland cement is one of the most used building materials in the world. Portland cement was used as a binding material in concrete production. It is known that around 4.1 billion tons of Portland cement is produced worldwide in 2020 [1]. In the production of Portland cement, a significant amount of carbon dioxide is released into the atmosphere and high energy consumption is caused [2–6]. According to the research, approximately 0.9 tons of carbon dioxide emissions occur for every one ton of Portland cement produced [7, 8]. With these values, Portland cement production alone is responsible for 5–7% of worldwide carbon dioxide [2, 7, 9–11]. In addition, approximately 5–12% of the energy used in production facilities in the world is spent on Portland cement production [10]. In our world, where the need for shelter is increasing, Portland cement production is increasing day by day, and in parallel to this increase, both carbon dioxide emissions and energy consumption are increasing worldwide. For this reason, researchers are investigating ways to develop new alternative binders in order to eliminate and/or reduce the unfavorable effects caused by the high use of Portland cement.

One of the alternative systems to Portland cement as a binder is geopolymer [12–14]. Geopolymers are a new class of inorganic polymer synthesized by activating of an aluminosilicate source with an alkaline hydroxide or silicate solution, which Davidovits first developed in the late 1970s [15–17]. In the production of geopolymers, waste/inert materials, such as fly ash and blast furnace slag are generally used as binding materials and have low CO_2 emission [6, 14, 18–27] Therefore, geopolymer systems are known as economical and environmentally friendly products [3, 28, 29]. When the geopolymer systems produced using fly ash are examined in the literature, it is observed that fly ash-based geopolymer systems can gain strength between 20 and 120 MPa with 24–72 h of heat curing at temperatures of 50–120 °C for different alkali activator ratios [3, 23, 30–38].

Moreover, it has been reported that fly ash-based geopolymers are generally more durable and have higher compressive strength than that of Portland cement [39, 40]. However, the energy spent for heat curing conditions is a disadvantage for fly ash-based geopolymer systems. For this reason, researchers have conducted studies in fly ash-based geopolymer systems with nano- and/or micro-particles such as SiO_2 [41–44], Al_2O_3 [16, 45, 46], TiO_2 [47], $CaCO_3$ [28] etc. to obtain higher strength at lower temperatures by reducing the heat curing time and/or temperature.

On the other hand, as it is known that the structure of geopolymer systems consists of Si–O-Al bonds [48]. While there is a high amount of Si (50–60%) in class F fly ash used, the Al content is in the range (15–25%). Therefore, the Al amount was thought to be less than that of necessary for complete geopolymeric reaction since each Si atom needs one Al atom. Thus, it was postulated that the number of bonds could be increased by adding some Al to the system to employ extra Si atom. The laboratory study was carried out to prove the above postulation.

Therefore, the influence of the addition of micronized aluminum powder in a fly ash-based geopolymer system was investigated in the current study. By providing extra bond between Si and Al atoms, it was aimed to obtain higher strength and better properties in a shorter time and at lower heat curing temperature by substituting the fly ash with aluminum powder. Within the scope of the study, 1, 2, and 3% aluminum powder was replaced with fly ash. Geopolymer mortar samples activated with sodium hydroxide were heat cured at 60, 70, and 80 °C temperatures for 24 and 48 h. The mini flow workability, unit weight, flexural, and compressive strength of the geopolymer mortar samples after heat curing was measured. Furthermore, field emission scanning electron microscopy (FESEM) examinations, X-ray diffraction (XRD), and Energy Dispersive X-Ray (EDX) analyses and reaction kinetics of geopolymerization were carried out to reveal the effects of aluminum powder on the microstructure. As a result of the study, the intended goals were achieved and it was seen that the physical, mechanical, and microstructure properties of fly ash-based geopolymer mortars could be improved with Al substitution.

Experiment parameters and test details

Materials

Class F fly ash with a specific gravity of 2.34 was used as a binder in the study. Chemical composition, SEM image, and XRD analysis of fly ash are presented in Table 1, Fig. 1, and Fig. 2, respectively. Micronized aluminum powder with a specific gravity of 2.69 was used by replacing with fly ash by weight. The chemical composition, SEM image, and XRD analysis, of the aluminum particles are presented in Table 2, Fig. 1, and Fig. 2, respectively. Solid sodium hydroxide particles were mixed with water and an alkali solution was obtained. Then, the prepared alkali solution was used for the production of geopolymer mortar. Standard Rilem sand

Table 1 Chemical compositions of fly ash (%)

Oxide	SiO_2	Al_2O_3	Fe_2O_3	CaO	SO_3	Na_2O	K_2O	MgO	LOI	Others
Fly Ash	59.11	21.8	8.15	2.91	0.61	1.6	1.8	1.98	0.96	1.08

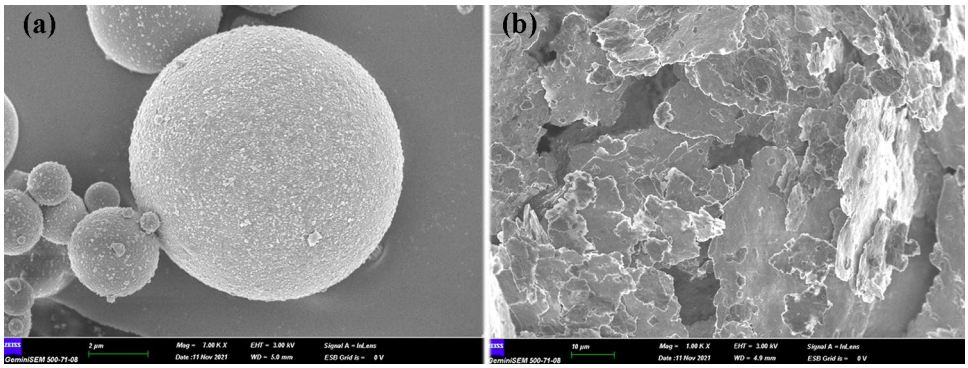

Fig. 1 SEM images of fly ash (7000x) and aluminum (1000x) (**a** fly ash, **b** aluminum)

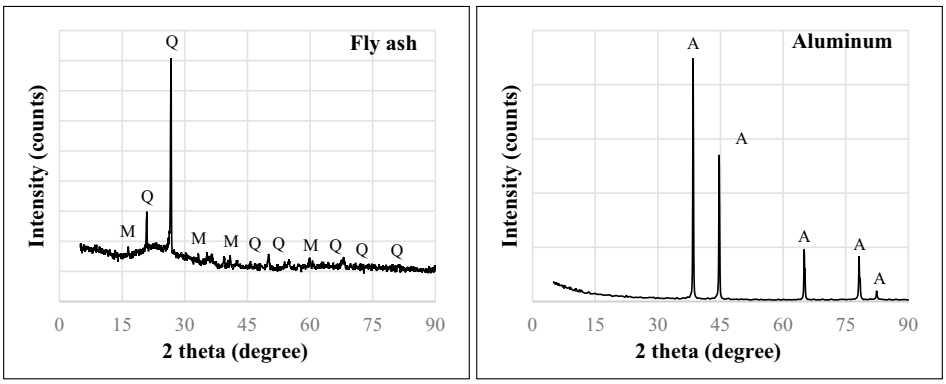

Fig. 2 XRD of fly ash and aluminum (*Q* Quartz, *M* Mullite, *A* Aluminum)

Table 2 Chemical compositions aluminum powder (%)

Element	Al	Fe	Si	S	Mg	LOI	Others
Aluminum	97.46	0.59	0.40	0.13	0.26	0.95	0.21

Table 3 Chemical ingredients of NaOH (%)

NaOH	Na_2CO_3	CI	Al	Fe	SO4
98.56	1.39	0.02	0.01	0.01	0.01

according to TS EN 196–1 [49] standard was used in the production of the geopolymer mortar. The chemical composition of sodium hydroxide is presented in Table 3.

Mixture design and detail

In the study, aluminum particles were used by replacing fly ash at the dosages of 0, 1, 2, and 3% by weight. The water/binder ratio was taken as 0.31, and the sand/binder ratio was taken as 3 for the geopolymer mortars. Alkali activator ratios as Na amount were 6, 8, and 10% of fly ash amount in mass basis. The mix proportion of geopolymer mortars are presented in Table 4.

Table 4 Mix proportion

Specimens	Fly ash	Aluminum	Aggregate	Na^+ ratio	Water	Heat curing condition	Heat curing time
	g	g	g	%	g	°C	Hour
Reference	450.0	0	1350	6-8-10	140	60-70-80	24–48
1% Al	445.5	4.5	1350	6-8-10	140	60-70-80	24–48
2% Al	441.0	9.0	1350	6-8-10	140	60-70-80	24–48
3% Al	436.5	13.5	1350	6-8-10	140	60-70-80	24–48

Fresh geopolymer mortars were prepared by mixing alkali solution with fly ash, aluminum powder, and standard Rilem sand. After the production of geopolymer mortars, the workabilities of the mortars were measured. Then, the fresh geopolymer mortars were placed in molds with which were three cell prisms having the dimensions of 160 × 40 × 40 (length, depth, and height) mm using vibration table. Geopolymer mortar specimens were heat cured at 60, 70, and 80 ℃, for 24 and 48 h in a laboratory oven. The specimens were not sealed during the heating. After heat curing, visual observation showed that there was no significant drying up damage on the samples. Following heat curing, the geopolymer mortar samples were taken out from mold and rested in the laboratory before testing until they reached a temperature of 23 ± 2 ℃.

Testing

Workability and unit weight

A flow test was carried out according to TS EN 1015–3 [50] specification. According to the relevant standard, the flow diameter value is defined as the average of the flow measurement value in two perpendicular directions of fresh mortar. Following the heat curing process, samples weights were measured and divided by their geometric dimensions and unit weight of geopolymer samples was determined.

Flexural and compressive strength

A three-point loading test was utilized to measure the flexural strength on three prismatic specimens, according to the TS EN 1015–11 [51] standard for each mixture. After the flexural test, the compressive strength test was carried out using six broken pieces according to the TS EN 1015–11 [51] standard. Flexural and compressive strength results were calculated as an average of the three and six specimens, respectively, for each mixture.

Microstructural characterization analysis (FESEM and EDX)

After heat curing at 60, 70, and 80 ℃, the geopolymer prism specimens were broken and the middle parts were used for the FESEM analyses. The examination was carried out by using Zeiss GeminiSEM electron microscopy. The samples were placed in the device and dried using infrared light for 5 min. The examinations were performed on the fractured surfaces of specimens in a vacuumed environment. Furthermore, EDX analyses were performed during FESEM analysis from designated areas.

X-ray diffraction (XRD) analysis

After heat curing, the specimens were powdered and sieved under 63 micron. Then, XRD analyzes were carried out on the powder samples obtained using a Bruker AXS D8 Advance device.

Isothermal conduction calorimetry

The reaction kinetics of the geopolymer mortars with and without Al were analyzed using isothermal calorimetry (TAM Air, TA Instruments Inc.,). In the experiment, 0, 1, 2, and 3% Al substituted geopolymer paste samples were produced with containing 10% Na activator. In order to examine the geopolymerization reaction, the paste samples were kept in an isothermal calorimeter device at 70 °C for 48 h.

Result and discussion

Workability and unit weight

The workability results of the fresh geopolymer mortar samples are presented in Fig. 3. It is a closer observation Fig. 3 showed that the workabilities of fresh reference geopolymer mortars containing 6, 8, and 10% Na^+ were 104, 107, and 115 mm, respectively. Furthermore, the workabilities of fresh geopolymer mortars containing 1% aluminum powder and activated with 6, 8, and 10% Na^+ were 103, 105, and 110 mm, respectively. Moreover, the workabilities of fresh geopolymer mortars containing 2% aluminum powder and activated with 6, 8, and 10% Na^+ were 102, 104 and 107 mm, respectively. Similarly, the workabilities of fresh geopolymer mortars containing 3% aluminum powder and activated with 6, 8, and 10% Na were 102, 103, and 106 mm, respectively.

Comparisons of workabilities made between the reference and aluminum powder containing geopolymer mortar showed that the workability of the geopolymer mortar samples increased with an increased amount of alkali activator. Fly ash particles are surrounded by Na^+ ion. Neighboring fly ash particles surrounded by Na^+ repel each other because the same charged molecule surrounds them. Therefore, agglomeration of fly ash particles is prevented and a workable mixture is obtained. This effect increases with increasing Na^+ content. Similar results have been found from other published articles [28, 52, 53]

However, the addition of aluminum decreased the workability of the fresh geopolymer mortar samples in comparison to the workability of the reference mortar. With the increasing amount of use of aluminum powder, a decrease in the workability values were observed at all sodium activator ratios.

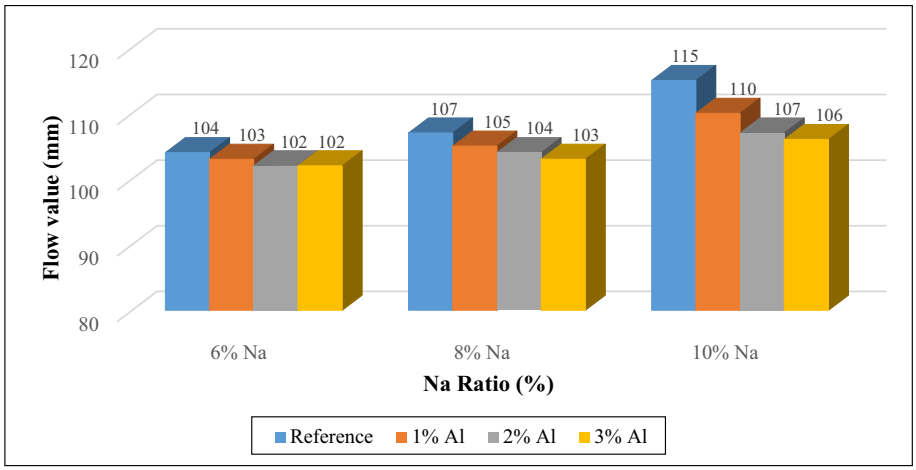

Fig. 3 Workability of fresh geopolymer mortar

Unit weight values of hardened geopolymer mortar samples are presented in Fig. 4. It is observed that the unit weight values of geopolymer mortar samples increased with the increasing use of activator substitution. For constant amount of aluminum powder, the increase in sodium amount result with higher unit weight. This is explained that more sodium concentration caused better workability thus resulting better compaction of fresh geopolymer mortar. For a constant sodium concentration, the increase in aluminum powder amount in geopolymer mortar gave slightly lower unit weight comparison to control mortar. This is explained by the fact that when fly ash, sodium hydroxide, and aluminum are mixed together, a rapid aluminum reaction starts and hydrogen gas creates a small void inside the mixture. However, since the presence of sand in the mixture increases the volume, this rapid reaction slows down and the amount of void that will be formed becomes insignificant. As a result, the difference between the unit weight of reference geopolymer mortar and geopolymer mortar containing aluminum can be considered negligible.

Compressive and flexural strengths

The compressive and flexural strengths of 0, 1, 2, and 3% aluminum substituted geopolymer mortar samples, which were heat cured at 60, 70 and 80 ℃ for 24 and 48 h, are given in Fig. 5, 6, 7 and Fig. 8, respectively. Based on the results, an increase in the compressive and flexural strengths of almost all samples is observed with the increase of heat curing temperature, heat curing time, and amount of activator, separately. In addition, all chemical processes were accelerated with increasing temperature. Increasing the heat curing time and temperature provides a more suitable environment for the formation of geopolymer gels [3, 28]. It is known that all chemical processes take place in time; therefore, increasing curing time increases the amount of geopolymeric gel formation. Moreover, an increase of activator concentration can dissolve more raw materials and increase the amount of geopolymeric gel formed. As a result, compressive and flexural strengths of geopolymer mortars increase [16, 31, 36, 38, 54–57].

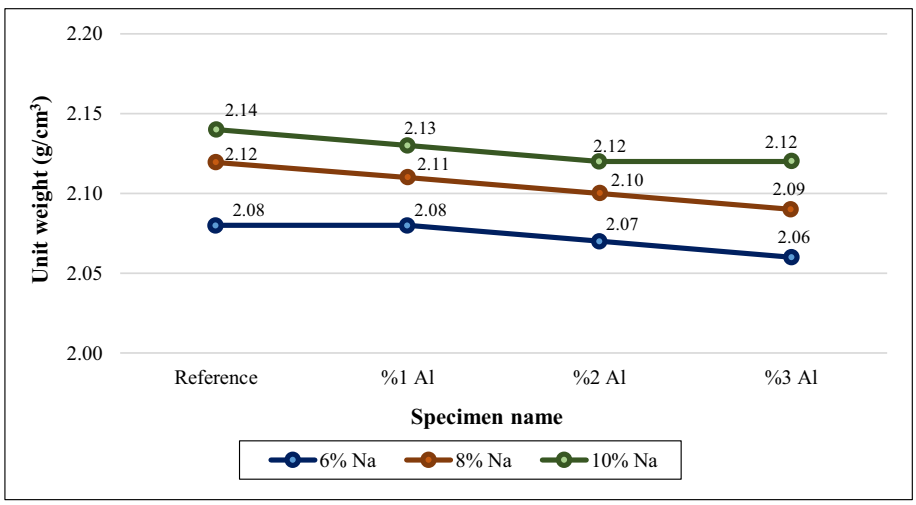

Fig. 4 Unit weight of mortars

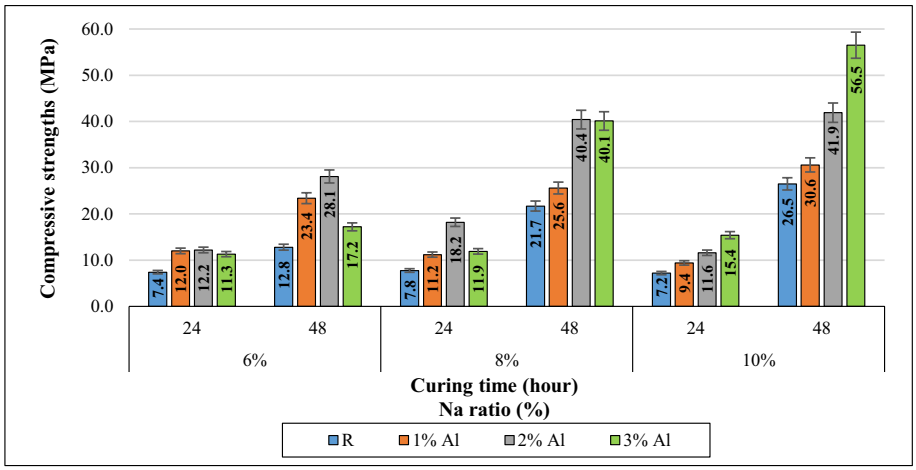

Fig. 5 Compressive strength of mortars after 60 ℃ heat curing temperature

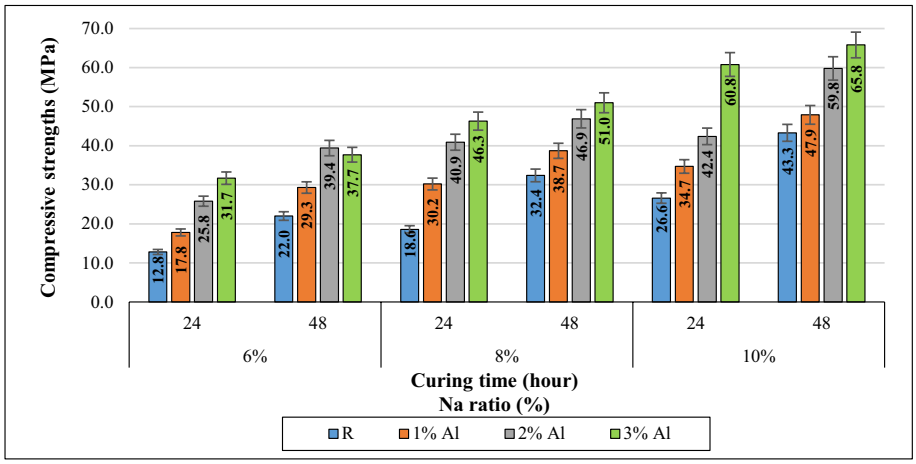

Fig. 6 Compressive strength of mortars after 70 ℃ heat curing temperature

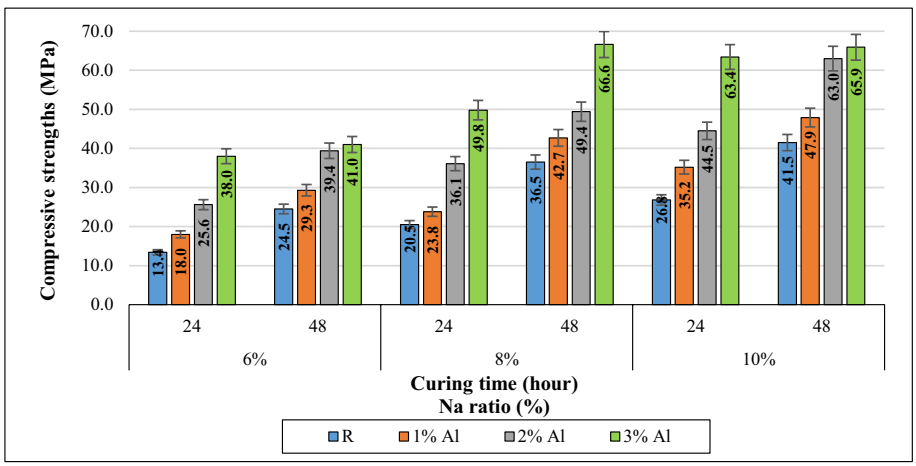

Fig. 7 Compressive strength of mortars after 80 ℃ heat curing temperature

However, it was determined that the aluminum particles used by replacing with fly ash in the ratios of 1, 2, and 3% significantly increased the compressive and flexural strengths of the geopolymer mortar samples.

After 60 ℃ heat curing, the compressive and flexural strengths of the geopolymer mortar samples containing 1, 2, and 3% aluminum were increased by 83, 235, 213, and 30, 56, 74%, respectively, compared to the reference sample.

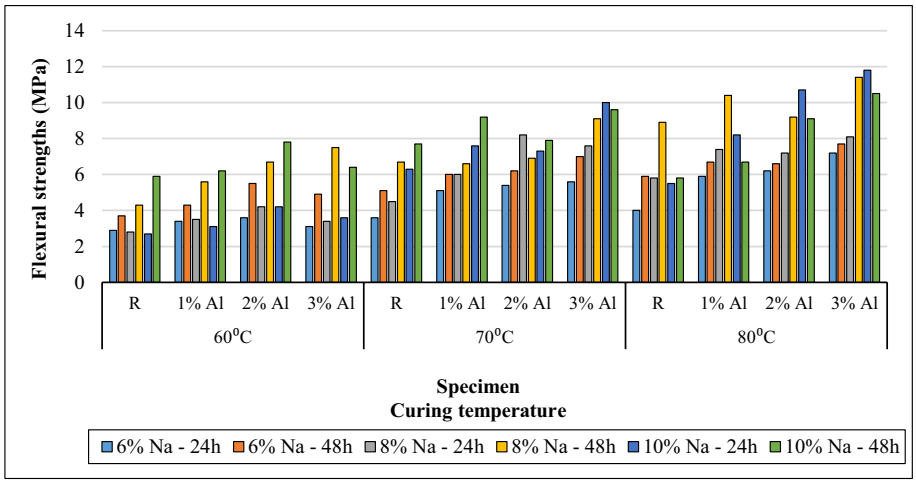

Fig. 8 Flexural strength of mortars

Similarly, after 70 ℃ heat curing, the compressive and flexural strengths of the geopolymer mortar samples containing 1, 2, 3% aluminum were increased by 62, 220, 249, and 42, 82, 69%, respectively, compared to the reference sample. Moreover, in the samples cured at 80 °C, with 1, 2, and 3% aluminum substitution, an increase in compressive and flexural strengths of 34, 91, 284, and 49, 95, 215%, respectively, was observed compared to the reference sample.

According to the strength test results, it was found that an increase of compressive strengths of more than two times can be achieved by substituting aluminum in samples of geopolymer mortar based on fly ash. For example, the compressive strength of 8% Na containing reference geopolymer mixture cured at 70 ℃ for 24 and 48 h are 18.6 MPa and 32.4 MPa. Extra 24 h heat curing results with 74% increase in compressive strength. On the other hand, the compressive strength of 8% Na containing geopolymer mixture made with 3% aluminum addition cured at 70 ℃ for 24 h is 46.3 MPa. Addition of 3% aluminum in the geopolymer mixture resulted with 134% increase in compressive strength in comparison to reference geopolymer mixture cured for 24 h. Moreover, the compressive strength of 3% aluminum added geopolymer mortar for 24 h of heat curing was 43% higher than the compressive strength of reference geopolymer mortar heat cured for 48 h. Aluminum addition seems to be more effective in improving strength than that of extra heat curing. With aluminum powder substitution, at the end of the 24 h heat curing period, it was seen that higher strengths could be obtained than the strengths of the reference samples without aluminum addition could reach with 48 h heat curing. Usage of aluminum powder in geopolymer matrix has resulted with significant energy and time-saving.

Although Duxson [58] and Songpiriyakij [59] reported that increasing the Si/Al ratio increases the compressive strength of geopolymer samples, the current study showed that decreasing the Si/Al ratio by addition of extra aluminum powder in the geopolymer mortar mixture remarkably increased the compressive and flexural strengths of geopolymer mortar more than two times in comparison to the reference mixture.

In addition, an attempt was made to relate compressive and flexural strength of geopolymer mortars, the relationship between flexural and compressive strengths obtained after 24 and 48 h of heat curing is presented in Fig. 9. It was determined that there is a strong relationship between flexural and compressive strengths with $R^2 = 0.89$ at the end of the 24 h heat curing period. However, $R^2 = 0.69$ for the relationship between flexural and compressive strengths was determined after 48 h of heat curing. This shows that the increase in compressive strength is higher than the flexural strength as the heat curing time increases. In other words, the increase in heat curing time results in a geopolymer mortar with higher compressive strength. However, the structure of geopolymer becomes more brittle with increasing heat curing time and the flexural strengths could not increase as much as compressive strength.

XRD analysis

XRD analysis results of reference 1, 2 and 3% Al substituted geopolymer powder samples heat cured at 70 ℃ for 24 h, are presented in Fig. 10. It is observed from the XRD analysis results that quartz (SiO_2), mullite ($Al_6Si_2O_{13}$), and albite ($NaAlSi_3O_8$) minerals were detected in the reference geopolymer samples [17, 27]. In addition, sodalite ($Na_4Al_3Si_3O_{12}OH$) minerals were detected in geopolymer samples with aluminum substitution. The dominant peak in the structure was the quartz peaks detected around 2 theta 26–27°. In geopolymer samples containing aluminum, quartz and mullite peaks were observed in 2 theta at 21, 26, 27, 36, 39, 43, 50, 60, 68, and 33, 41, respectively, as in the reference sample. In addition, there is a scattered wide peak between 20 and 41 that designates the evolution of N-A-S–H gel with amorphous character [38, 60]. Moreover, it

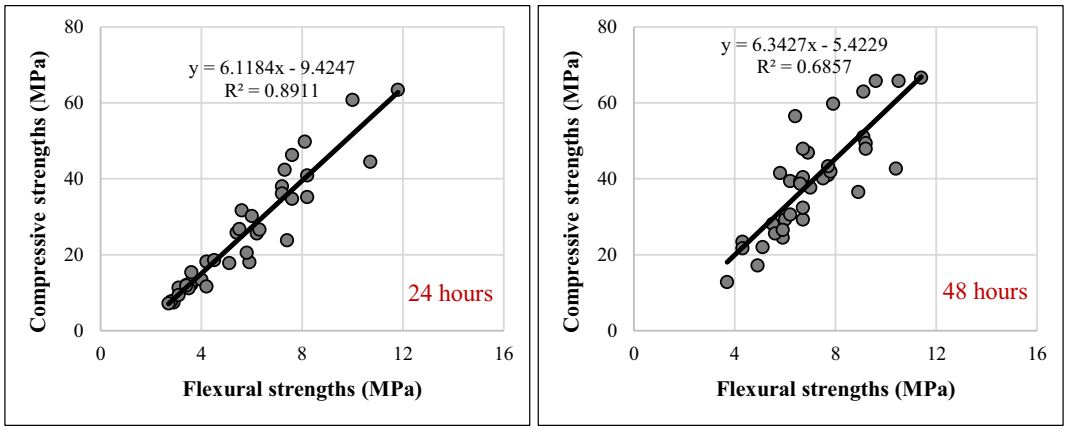

Fig. 9 Relationship between flexural and compressive strengths

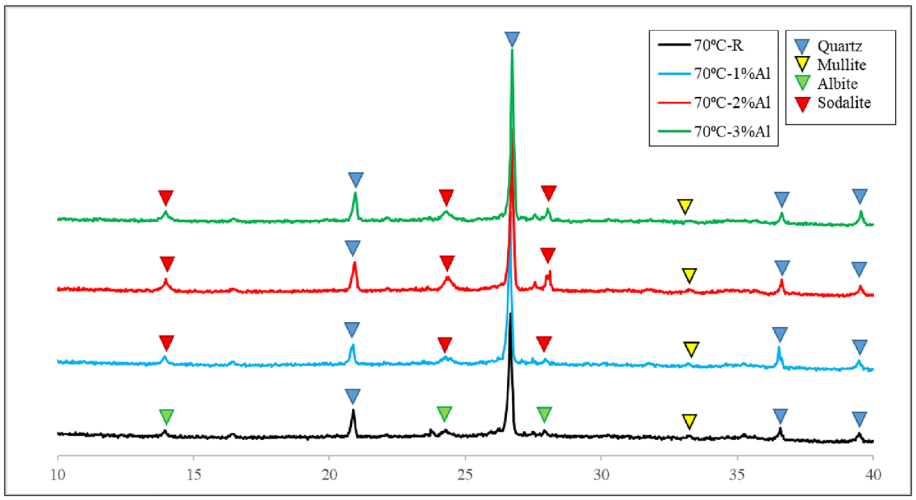

Fig. 10 XRD analysis of geopolymer samples (2 Theta (°))

was observed that the Albite peaks detected in 2theta 13.94, 23.73, and 26.65 in the reference sample were transformed into sodalite peaks for geopolymer made with Al substitution. For sodalite peaks, 2theta values were detected 14.02, 24.32, and 26.73 ICDD number of Albite and Sodalite were 00–009-0466 and 01–076-1639, respectively. When the chemical composition of albite ($NaAlSi_3O_8$) and sodalite ($Na_4Al_3Si_3O_{12}OH$) minerals are examined, it is observed that more aluminum is needed for sodalite formation.

The formation of sodalite minerals instead of albite minerals with Al substitution can be considered as an indication that aluminum powders participate in the geopolimeric reactions. Moreover, it is thought that sodalite formation increases the strength of the geopolymer mortar. Chen et al. [38], studied on 'The effect on the compressive strength of fly ash-based geopolymer concrete with the generation of hydroxy sodalite'. They stated that at the appropriate amount of sodium hydroxide and aluminum content in the mixture the hydroxy sodalite was formed during heat curing. Thus, the formation of hydroxide sodalite and N-A-S-H generation leads to high strength. They concluded that the highest compressive strength can be attributed to the generation of N-A-S-H gel and hydroxy sodalites. Moreover, Sathishraj Mani and Bulu Pradhan [61] made a parallel conclusion by stating that the higher compressive strength is attributed to a higher amount of sodium aluminosilicate hydrate (NA-S-H) gel formation through albite phase and predominant zeolite phases such as gismondine and sodalite.

FESEM-EDX analysis

FESEM images of geopolymer samples are presented in Fig. 11. It is observed from Fig. 11 that the geopolymer samples turn into a compact structure with low porosity due to an increase in the heat curing temperature and aluminum substitution. FESEM pictures of the 60C-R and 80C-R samples are presented in Fig. 12a,b respectively, to examine the influence of heat curing temperature in detail. Many

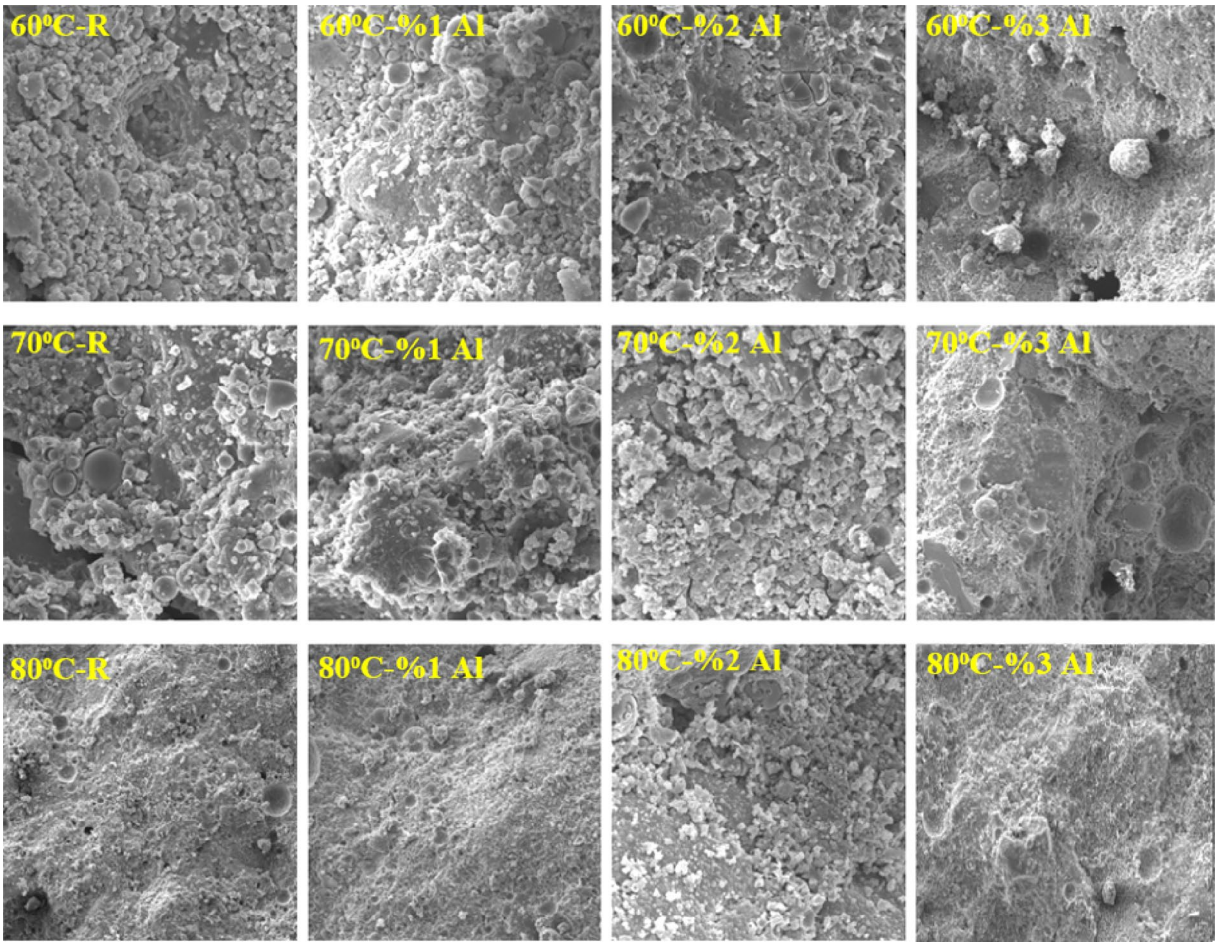

Fig. 11 FESEM images of geopolymer mortars (500x)

spherical unreacted or partially reacted particles, which are thought to be fly ash particles, are observed in Fig. 12a. The EDX analysis results on these spherical particles are presented in Fig. 12 as EDX-1. According to the results obtained, it was concluded that the chemical composition of these structures is very similar to the chemical composition of fly ash. Therefore, these particles were defined as fly ash. Furthermore, when Fig. 12b (80 ℃-R) is examined, it is observed that the amount of unreacted fly ash grains decreases, and the microstructure turns into a more compact structure with an increase in heat curing temperature. The microstructure becomes denser with the increase of heat curing temperature and the higher amount of the reacted fly ash particles are seen as the influencing parameter that contributes to the increase of the strength values due to the effect of heat curing. In the EDX-2 analysis performed in Fig. 12b, the presence of silica, aluminum, and sodium was determined in accordance with the N-A-S–H structure seen in the fly ash-based geopolymer samples [62, 63]. While the amount of silica detected in the matrix structure of the reference sample was (26.67%), the amount of aluminum was determined as (12.52%). The rate of Si/Al is found to be compatible with the amount of 59.11% silica and 21.8% aluminum in the chemical composition of fly ash.

On the other hand, to observe the changes in the microstructure with aluminum substitution, the microstructures of the samples with 3%Al substitution were examined under 20,000×magnification. As a result of the examinations, the appearance of the matrix structures in two different regions on the fly ash surface in the microstructure and EDX analyzes are presented in Fig. 13. The needle or rod-like structures observed in Fig. 13 are thought to be sodalite structures (similar sodalite appearances are encountered in the literature [38, 64]), whose presence was also detected in the XRD analysis. The EDX-3 and EDX-4 analyses were carried out to determine the chemical composition of the detected rod-like structures. The obtained results showed that the amounts of aluminum (20.58%) and silica (21.64%) in the chemical composition of the rod-like structure matrices were almost equal. These results are also compatible with the chemical formula of sodalite ($Na_4Al_3Si_3O_{12}OH$). The amount of silica

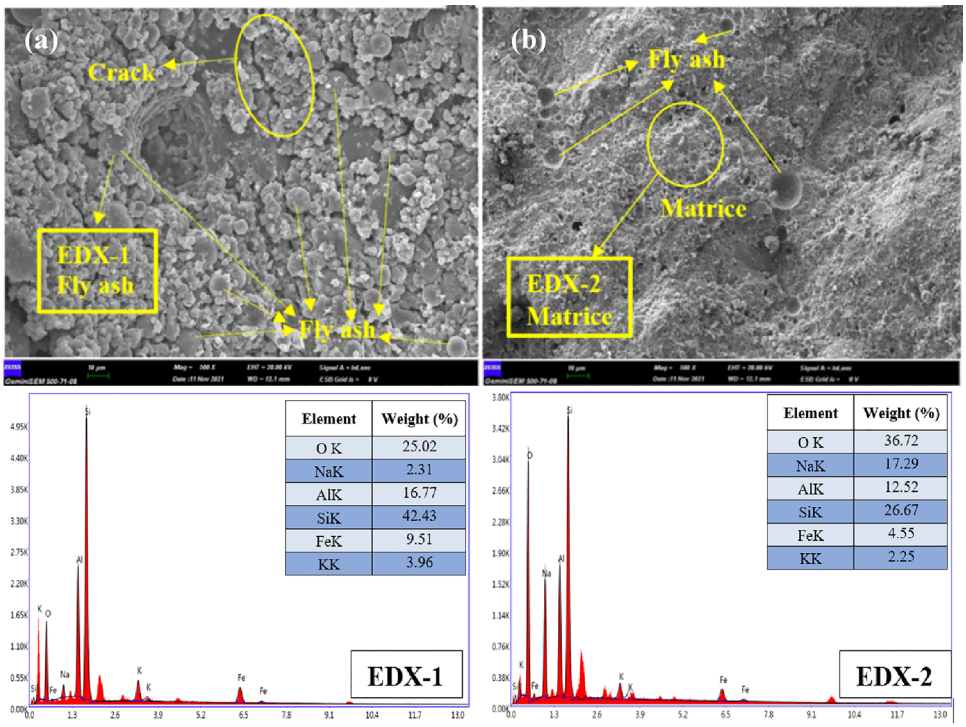

Fig. 12 EDX and SEM image (500x) of fly ash and geopolymer matrix

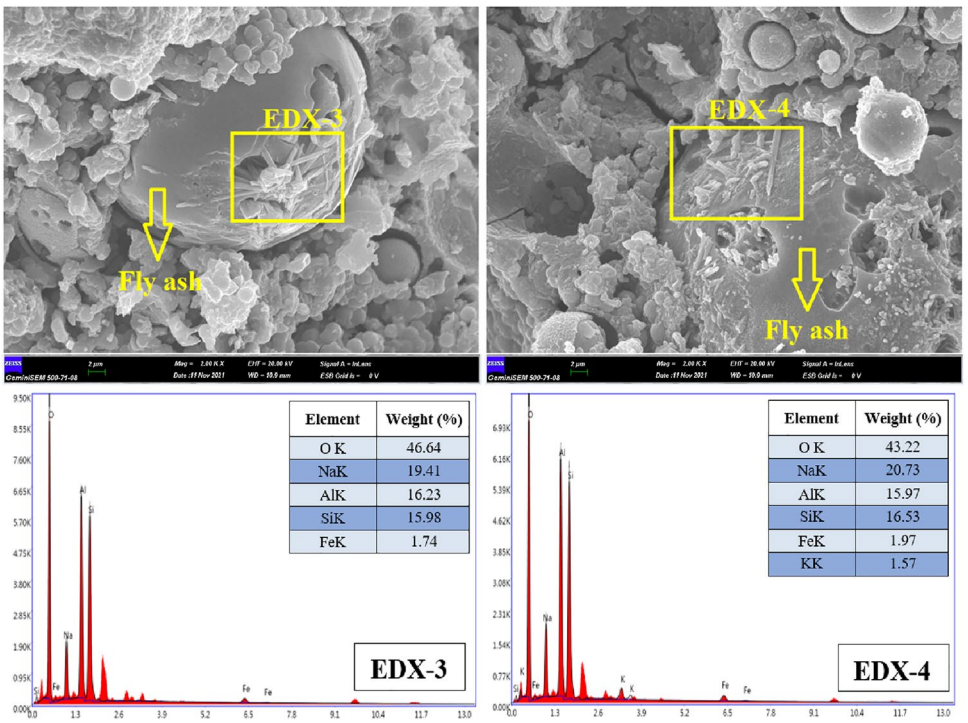

Fig. 13 EDX and SEM images (2000x) of fly ash and aluminum reaction matrix

detected in the reference geopolymer matrices is more than the amount of aluminum. However, the amount of aluminum in the matrix structure of the samples with aluminum substitutes is almost equal to that of silica is considered as an indication that the aluminum included in the system participates in the reactions and forms a new structure. Moreover, it is thought that sodalite with rod-like structure, which is thought to be formed in the matrix with aluminum substitution, contributes to the increase in compressive and flexural strengths [38]. Furthermore, it

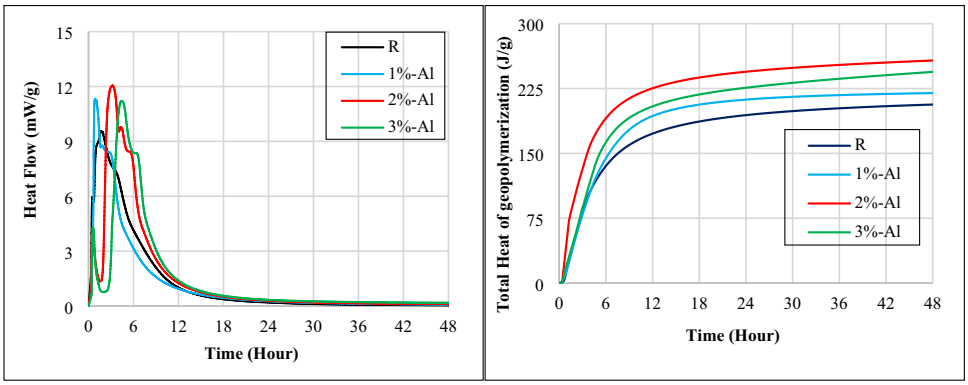

Fig. 14 Rate of and cumulative heat of geopolymerization at 70 ℃

might be concluded that the strengths increase as a result of the interlocking of the needle-shaped sodalite structures seen in Fig. 13.

Geopolymerization kinetic

Heat curves of the geopolymerization reaction obtained using reaction kinetic analysis of the control and aluminum powder containing pastes (at 1, 2, and 3% substitution ratio) at 70 ℃ are given in Fig. 14.

When the heat flow accelerations are examined, it is observed that the heights of rate peaks increased with aluminum substitutions. The peak position also changed in time scale compared to the reference sample (1.8 h), the aluminum containing samples took different times to reach acceleration peaks (1.0 h for 1%-Al, 4.4 h for 2%Al and 3.2 h for 3%Al) In addition, increasing aluminum substitution was elevated the rate of peaks. The maximum peak was obtained from 3% aluminum substitution. It is known that the higher the rate of specimen peak results with a high amount of reaction product, which is associated with sample hardening and strength development [28, 60].

The total heat of geopolymerization curves are presented in Fig. 14. It is observed that the total heat of geopolymerization is 207 J/g for the reference sample. Furthermore, the total heat of geopolymerization for 1%, 2% and 3% aluminum substitution rates are 220 J/g, 243 J/g and 257 J/g. It can be seen that increasing substitution of aluminum, increased the total heat of geopolymerization. It is attributed that the total heat released during the geopolymerization reaction of the samples can give an explanation for both the formation of the reaction product and the strength development [60]. The contributions of aluminum substitution to the rate and the heat of reactions Querydiscussed above are in agreement with compressive and flexural strength results. The significant contribution of aluminum to the strengths of geopolymer mortars was observed for the first 24 h of heat curing. This is found to be in line with the evident effects of aluminum on the rate of heat flows and total heat of geopolymerization curves.

Conclusions

1. The workability of fresh geopolymer mortars increased with the increase of sodium content. Negligible decreases in workability were observed with aluminum substitution.
2. Increasing the sodium content increased the unit weights of the hardened geopolymer mortar samples. However, increasing the aluminum slightly decreased the unit weights of the hardened geopolymer mortar samples.
3. The increase in sodium content, aluminum substitution, heat curing temperature, and heat curing time increased the compressive, and flexural strength values of the hardened geopolymer mortar samples.
4. More than one hundred percent increases were obtained in the compressive and flexural strength of class F fly ash-based geopolymer mortar samples with aluminum replacement. These increases are attributed to sodalite formation in the microstructure.
5. As a result of XRD analysis, it was observed that albite minerals detected in the reference sample were transformed into sodalite minerals with aluminum substitution.
6. According to FESEM images, it was observed that a rod-like sodalite structure was formed in the microstructure with aluminum substitution. It has been observed that these structures improve the mechanical properties by resulting in better microstructures.
7. It was concluded that the total heat of geopolymerization increased with the substitution of aluminum. This shows that aluminum took part in the geopolymerization reactions, thus resulting in higher strength in comparison to the reference samples.

Author contribution UD literature search, investigation, experiment and writing.

Funding This work did not receive any specific grant from any funding agencies.

Data availability No data used.

Declarations

Conflict of interests The authors declare no conflict of interests.

Ethical approval Not applicable.

Consent for publication Not applicable.

References

1. Garside M (2021) Statista. https://www.statista.com/statistics/1087115/global-cement-production-volume/
2. Bildirici ME (2020) The relationship between cement production, mortality rate, air quality, and economic growth for China, India, Brazil, Turkey, and the USA: MScBVAR and MScBGC analysis. Environ Sci Pollut Res 27:2248–2263. https://doi.org/10.1007/s11356-019-06586-w
3. Atiş CD, Görür EB, Karahan O et al (2015) Very high strength (120 MPa) class F fly ash geopolymer mortar activated at different NaOH amount, heat curing temperature and heat curing duration. Constr Build Mater 96:673–678. https://doi.org/10.1016/j.conbuildmat.2015.08.089
4. Çelikten S, Sarıdemir M, Özgür Deneme İ (2019) Mechanical and microstructural properties of alkali-activated slag and slag + fly ash mortars exposed to high temperature. Constr Build Mater 217:50–61. https://doi.org/10.1016/j.conbuildmat.2019.05.055
5. Andrew RM (2018) Global CO2emissions from cement production. Earth Syst Sci Data 10:195–217. https://doi.org/10.5194/essd-10-195-2018
6. Moni SMFK, Ikeora O, Pritzel C et al (2020) Preparation and properties of fly ash-based geopolymer concrete with alkaline waste water obtained from foundry sand regeneration process. J Mater Cycles Waste Manag 22:1434–1443. https://doi.org/10.1007/s10163-020-01032-3
7. Benhelal E, Zahedi G, Shamsaei E, Bahadori A (2013) Global strategies and potentials to curb CO2 emissions in cement industry. J Clean Prod. https://doi.org/10.1016/j.jclepro.2012.10.049
8. Mahasenan N, Smith S, Humphreys K (2003) The cement industry and global climate change: current and potential future cement industry CO_2 emissions. In: Greenhouse gas control technologies - 6th international conference, Kyoto, Japan, Vol II, Pages 995–100, Pergamon. https://doi.org/10.1016/B978-008044276-1/50157-4
9. Chen W, Hong J, Xu C (2015) Pollutants generated by cement production in China, their impacts, and the potential for environmental improvement. J Clean Prod 103:61–69. https://doi.org/10.1016/J.JCLEPRO.2014.04.048
10. Ali MB, Saidur R, Hossain MS (2011) A review on emission analysis in cement industries. Renew Sustain Energy Rev. https://doi.org/10.1016/j.rser.2011.02.014
11. Deja J, Uliasz-Bochenczyk A, Mokrzycki E (2010) CO2 emissions from Polish cement industry. Int J Greenh Gas Control. https://doi.org/10.1016/j.ijggc.2010.02.002
12. Kaya M (2022) The effect of micro-SiO2 and micro-Al2O3 additive on the strength properties of ceramic powder-based geopolymer pastes. J Mater Cycles Waste Manag 24:333–350. https://doi.org/10.1007/s10163-021-01323-3
13. Cai J, Li X, Tan J, Vandevyvere B (2020) Thermal and compressive behaviors of fly ash and metakaolin-based geopolymer. J Build Eng 30:101307. https://doi.org/10.1016/j.jobe.2020.101307
14. Mishra J, Nanda B, Patro SK et al (2022) Influence of ferrochrome ash on mechanical and microstructure properties of ambient cured fly ash-based geopolymer concrete. J Mater Cycles Waste Manag 24:1095–1108. https://doi.org/10.1007/s10163-022-01381-1
15. Davidovits J (1991) Geopolymers - inorganic polymeric new materials. J Therm Anal. https://doi.org/10.1007/BF01912193
16. Huang Y, Han M (2011) The influence of α-Al_2O_3 addition on microstructure, mechanical and formaldehyde adsorption properties of fly ash-based geopolymer products. J Hazard Mater 193:90–94. https://doi.org/10.1016/j.jhazmat.2011.07.029
17. Azimi EA, Abdullah MMAB, Vizureanu P et al (2020) Strength development and elemental distribution of dolomite/fly ash geopolymer composite under elevated temperature. Materials (Basel). https://doi.org/10.3390/ma13041015
18. Palomo Á, Alonso S, Fernandez-Jiménez A et al (2004) Alkaline activation of fly ashes: nmr study of the reaction products. J Am Ceram Soc 87:1141–1145. https://doi.org/10.1111/j.1551-2916.2004.01141.x
19. Saxena R, Gupta T, Sharma RK, Siddique S (2022) Mechanical, durability and microstructural assessment of geopolymer concrete incorporating fine granite waste powder. J Mater Cycles Waste Manag 24:1842–1858. https://doi.org/10.1007/s10163-022-01439-0
20. Kumar S, Mucsi G, Kristály F, Pekker P (2017) Mechanical activation of fly ash and its influence on micro and nano-structural behaviour of resulting geopolymers. Adv Powder Technol 28:805–813. https://doi.org/10.1016/j.apt.2016.11.027
21. Bingöl Ş, Bilim C, Atiş CD, Durak U (2020) Durability properties of geopolymer mortars containing slag. Iran J Sci Technol Trans Civ Eng. https://doi.org/10.1007/s40996-019-00337-0
22. Chen-Tan NW, Van Riessen A, Ly CV, Southam DC (2009) Determining the reactivity of a fly ash for production of geopolymer. J Am Ceram Soc 92:881–887. https://doi.org/10.1111/j.1551-2916.2009.02948.x
23. Atabey I, Karahan O, Bilim C, Atiş CD (2020) Very high strength na2sio3 and naoh activated fly ash based geopolymer mortar. Cem Wapno Bet 2020:292–305. https://doi.org/10.32047/CWB.2020.25.4.4
24. Kaya M, Köksal F (2020) Effect of cement additive on physical and mechanical properties of high calcium fly ash geopolymer mortars. Struct Concr. https://doi.org/10.1002/suco.202000235
25. Durak U, İlkentapar S, Karahan O et al (2021) A new parameter influencing the reaction kinetics and properties of fly ash based geopolymers: a pre-rest period before heat curing. J Build Eng 35:102023. https://doi.org/10.1016/j.jobe.2020.102023
26. Benito P, Leonelli C, Medri V, Vaccari A (2013) Geopolymers a new and smart way for a sustainable development. Appl Clay Sci 73:1. https://doi.org/10.1016/j.clay.2013.03.008
27. Part WK, Ramli M, Cheah CB (2015) An overview on the influence of various factors on the properties of geopolymer concrete derived from industrial by-products. Constr Build Mater 77:370–395. https://doi.org/10.1016/j.conbuildmat.2014.12.065
28. Durak U, Karahan O, Uzal B et al (2021) Influence of nano SiO2 and nano CaCO3 particles on strength, workability, and microstructural properties of fly ash-based geopolymer. Struct Concr 22:E352–E367. https://doi.org/10.1002/suco.201900479
29. Das D, Rout PK (2021) Synthesis and Characterization of Fly Ash and GBFS Based Geopolymer Material. Biointerface Res Appl Chem. https://doi.org/10.33263/BRIAC116.1450614519
30. Saxena R, Gupta T (2022) Assessment of mechanical, durability and microstructural properties of geopolymer concrete containing ceramic tile waste. J Mater Cycles Waste Manag 24:725–742. https://doi.org/10.1007/s10163-022-01353-5
31. Chen K, Lin W-T, Liu W (2021) Effect of NaOH concentration on properties and microstructure of a novel reactive ultra-fine fly ash geopolymer. Adv Powder Technol 32:2929–2939. https://doi.org/10.1016/j.apt.2021.06.008
32. Criado M, Fernández-Jiménez A, de la Torre AG et al (2007) An XRD study of the effect of the SiO2/Na2O ratio on the alkali

activation of fly ash. Cem Concr Res 37:671–679. https://doi.org/10.1016/j.cemconres.2007.01.013
33. Andini S, Cioffi R, Colangelo F et al (2008) Coal fly ash as raw material for the manufacture of geopolymer-based products. Waste Manag 28:416–423. https://doi.org/10.1016/j.wasman.2007.02.001
34. Chithambaram SJ, Kumar S, Prasad MM, Adak D (2018) Effect of parameters on the compressive strength of fly ash based geopolymer concrete. Struct Concr 19:1202–1209. https://doi.org/10.1002/suco.201700235
35. Kaya M, Uysal M, Yilmaz K et al (2020) Mechanical properties of class c and f fly ash geopolymer mortars. J Croat Assoc Civ Eng. https://doi.org/10.14256/JCE.2421.2018
36. Rattanasak U, Chindaprasirt P (2009) Influence of NaOH solution on the synthesis of fly ash geopolymer. Miner Eng 22:1073–1078. https://doi.org/10.1016/j.mineng.2009.03.022
37. Guo X, Shi H, Dick WA (2010) Compressive strength and microstructural characteristics of class C fly ash geopolymer. Cem Concr Compos 32:142–147. https://doi.org/10.1016/j.cemconcomp.2009.11.003
38. Chen Z, Wan X, Qian Y et al (2021) The effect on the compressive strength of fly ash based geopolymer concrete with the generation of hydroxy sodalite. Constr Build Mater. https://doi.org/10.1016/j.conbuildmat.2021.125174
39. Nath SK, Maitra S, Mukherjee S, Kumar S (2016) Microstructural and morphological evolution of fly ash based geopolymers. Constr Build Mater 111:758–765. https://doi.org/10.1016/j.conbuildmat.2016.02.106
40. Hardjito D, Rangan BV (2005) Development and properties of low-calcium fly ash-based geopolymer concrete. Research report GC-1, Faculty of Engineering, Curtin University of Technology, Perth, Australia
41. Shaikh FUA, Supit SWM, Sarker PK (2014) A study on the effect of nano silica on compressive strength of high volume fly ash mortars and concretes. Mater Des 60:433–442. https://doi.org/10.1016/j.matdes.2014.04.025
42. Ibrahim M, Johari MAM, Maslehuddin M, Rahman MK (2018) Influence of nano-SiO2 on the strength and microstructure of natural pozzolan based alkali activated concrete. Constr Build Mater 173:573–585. https://doi.org/10.1016/j.conbuildmat.2018.04.051
43. Liu M, Tan H, He X (2019) Effects of nano-SiO2 on early strength and microstructure of steam-cured high volume fly ash cement system. Constr Build Mater 194:350–359. https://doi.org/10.1016/j.conbuildmat.2018.10.214
44. Supit SWM, Shaikh FUA (2015) Durability properties of high volume fly ash concrete containing nano-silica. Mater Struct 48:2431–2445. https://doi.org/10.1617/s11527-014-0329-0
45. Chindaprasirt P, De Silva P, Sagoe-Crentsil K, Hanjitsuwan S (2012) Effect of SiO 2 and Al 2O 3on the setting and hardening of high calcium fly ash-based geopolymer systems. J Mater Sci 47:4876–4883. https://doi.org/10.1007/s10853-012-6353-y
46. Phoo-ngernkham T, Chindaprasirt P, Sata V et al (2014) The effect of adding nano-SiO2 and nano-Al2O3 on properties of high calcium fly ash geopolymer cured at ambient temperature. Mater Des 55:58–65. https://doi.org/10.1016/j.matdes.2013.09.049
47. Duan P, Yan C, Luo W, Zhou W (2016) Effects of adding nano-TiO2on compressive strength, drying shrinkage, carbonation and microstructure of fluidized bed fly ash based geopolymer paste. Constr Build Mater 106:115–125. https://doi.org/10.1016/j.conbuildmat.2015.12.095
48. Dav J (1994) High-alkali cements for 21 sf century concretes. ACI Spec Publicaton 144(1994):382–398
49. En TS (2016) Methods of testing cement—part:1 determination of strength. TSE, Ankara, Turkey
50. En TS (2000) Methods of test for mortar for masonry: Part 3. TSE, Ankara, Turkey, Determination of consistence of fresh mortar (by flow table)
51. En TS (2020) Methods of test for mortar for masonry - Part 11: Determination of flexural and compressive strength of hardened mortar. TSE, Ankara, Turkey
52. Sathonsaowaphak A, Chindaprasirt P, Pimraksa K (2009) Workability and strength of lignite bottom ash geopolymer mortar. J Hazard Mater 168:44–50. https://doi.org/10.1016/j.jhazmat.2009.01.120
53. Nath P, Sarker PK (2014) Effect of GGBFS on setting, workability and early strength properties of fly ash geopolymer concrete cured in ambient condition. Constr Build Mater 66:163–171. https://doi.org/10.1016/j.conbuildmat.2014.05.080
54. Phavongkham V, Wattanasiriwech S, Wattanasiriwech D (2021) Tailored design of properties of hongsa fly ash-based geopolymer paste via an adjustment of the alkali activator composition. Ceram Int 47:13374–13380. https://doi.org/10.1016/j.ceramint.2021.01.194
55. De Vargas AS, Dal Molin DCC, Vilela ACF et al (2011) The effects of Na2O/SiO2 molar ratio, curing temperature and age on compressive strength, morphology and microstructure of alkali-activated fly ash-based geopolymers. Cem Concr Compos. https://doi.org/10.1016/j.cemconcomp.2011.03.006
56. Hadi MNS, Al-Azzawi M, Yu T (2018) Effects of fly ash characteristics and alkaline activator components on compressive strength of fly ash-based geopolymer mortar. Constr Build Mater 175:41–54. https://doi.org/10.1016/j.conbuildmat.2018.04.092
57. Kaur M, Singh J, Kaur M (2018) Synthesis of fly ash based geopolymer mortar considering different concentrations and combinations of alkaline activator solution. Ceram Int 44:1534–1537. https://doi.org/10.1016/j.ceramint.2017.10.071
58. Duxson P, Provis JL, Lukey GC et al (2005) Understanding the relationship between geopolymer composition, microstructure and mechanical properties. Coll Surf A Physicochem Eng Asp 269:47–58. https://doi.org/10.1016/j.colsurfa.2005.06.060
59. Songpiriyakij S, Kubprasit T, Jaturapitakkul C, Chindaprasirt P (2010) Compressive strength and degree of reaction of biomass- and fly ash-based geopolymer. Constr Build Mater 24:236–240. https://doi.org/10.1016/j.conbuildmat.2009.09.002
60. Ishwarya G, Singh B, Deshwal S, Bhattacharyya SK (2019) Effect of sodium carbonate/sodium silicate activator on the rheology, geopolymerization and strength of fly ash/slag geopolymer pastes. Cem Concr Compos 97:226–238. https://doi.org/10.1016/J.CEMCONCOMP.2018.12.007
61. Mani S, Pradhan B (2020) Investigation on effect of fly ash content on strength and microstructure of geopolymer concrete in chloride-rich environment. Mater Today Proc 32:865–870. https://doi.org/10.1016/j.matpr.2020.04.216
62. Puligilla S, Mondal P (2013) Role of slag in microstructural development and hardening of fly ash-slag geopolymer. Cem Concr Res 43:70–80. https://doi.org/10.1016/J.CEMCONRES.2012.10.004
63. Puertas F, Martínez-Ramírez S, Alonso S, Vázquez T (2000) Alkali-activated fly ash/slag cements: Strength behaviour and hydration products. Cem Concr Res 30:1625–1632. https://doi.org/10.1016/S0008-8846(00)00298-2
64. Novembre D, Gimeno D, Pasculli A, Di Sabatino B (2010) Synthesis and characterization of sodalite using natural kaolinite: an analytical and mathematical approach to simulate the loss in weight of chlorine during the synthesis process. Fresenius Environ Bull 19:1109–1117

Authors and Affiliations

Uğur Durak[1]

✉ Uğur Durak
ugurdurak@erciyes.edu.tr

[1] Civil Engineering Department, Engineering Faculty, Erciyes University, 38039 Kayseri, Turkey